

Convergent Proton-Transfer Photocycles Violate Mirror-Image Symmetry in a Key Melanin Monomer

Seth Olsen,^{*,†} Jennifer Riesz,[‡] Indu Mahadevan,[‡] Aaron Coutts,[‡] Jacques P. Bothma,[‡] Benjamin J. Powell,[‡] Ross H. McKenzie,[‡] Sean C. Smith,[†] and Paul Meredith[‡]

Centre for Computational Molecular Science, Australian Institute for Bioengineering and Nanotechnology, and
²Condensed Matter Group, School of Physical Sciences, The University of Queensland,
Brisbane, QLD 4072 Australia

Received December 25, 2006; E-mail: s.olsen1@uq.edu.au

We present evidence for mirror-image rule¹ violation in spectra of 5,6-dihydroxyindole-2-carboxylic acid (DHICA), a key melanin monomer, and propose that this phenomenon is due to convergent adiabatic and nonadiabatic excited-state intramolecular proton-transfer (ESIPT) processes. Specifically, excitation into the S_1 or S_2 states of a catechololate anion of DHICA, represented by dual bands in the absorption spectrum, leads to emission from the S_1 state of its proton-transfer conjugate. This suggests that intramonomer ESIPT may function as an energy dissipation mechanism in the macromolecular pigment.

Eumelanin, a subclass of melanin, is a major component of the human pigmentary system.^{2,3} It displays intriguing photophysics, including a broad, monotonically decreasing absorbance spanning the near UV, visible, and IR ranges, and efficient radiationless deactivation leading to ground-state regeneration with yield approaching unity.^{4,5}

Eumelanins are brown-black macromolecular pigments derived from 5,6-dihydroxyindole (DHI) and DHICA.³ The insolubility and heterogeneity of eumelanin make it a difficult material for experimental study. As a result, little is known about its structure–property relationships.^{6,7} DHICA is stable in solution, making it an important model compound for the indirect inference of these relationships in eumelanin.

Figure 1 displays the scaled absorption and emission spectra of DHICA in aqueous solution at pH 9.0. Descriptions of DHICA synthesis, purification, and spectroscopy are included in the Supporting Information. There is an absorption peak near 3.8 eV and a distinct shoulder near 4.2 eV; excitation into either of these bands leads to emission which peaks at 3.0 eV in the scaled emission. Mirror-image rule violation is manifest in the lack of a shoulder in the emission spectrum and a broadened width of the emission relative to the main absorption peak.

Acid–base dissociations in DHICA occur with pK_a 's at 4.25, 9.76, and 13.2.⁸ Comparison with DHI and catechol suggests that the second and third of these correspond to successive titration of the catecholic moiety. Strict identification with these sites is problematic because macroscopic pK_a 's of multiprotic acids with interacting sites do not correspond to individual site pK_a 's.⁹ Instead, they represent averages over all pathways connecting the ensembles with n and $n - 1$ protons. The spectra which we report were collected below the second macroscopic pK_a of DHICA, where the ratio of dianions to monoanions should be small. However, the proximity to the catechol-like pK_a mandates consideration of all possible DHICA monoanions in our analysis. These are displayed in Figure 2.

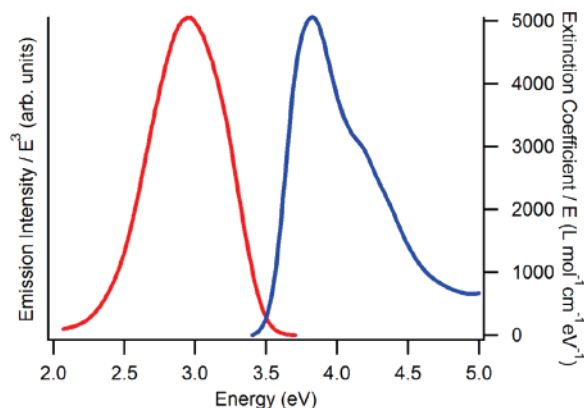


Figure 1. Scaled absorption (blue) and emission (red) spectra of DHICA in aqueous solution (borax buffer at pH 9.0).

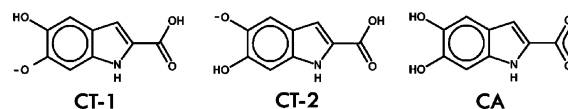


Figure 2. Three DHICA monoanions with nomenclature.

Of the catechololate anions, **CT-1** is uniformly predicted to be energetically preferred in the ground state. We have calculated the S_0 – S_1 and S_0 – S_2 transitions of **CT-1** and **CA** with equation-of-motion coupled cluster singles and doubles¹⁰ (EOM-CCSD) theory with a Dunning double- ζ basis set^{11,12} (polarization functions on heavy atoms). These calculations predict S_0 – S_1 and S_0 – S_2 transitions at 3.60 and 4.39 eV for **CT-1** and 4.47 and 4.79 eV for **CA**. The excited states have $\pi\pi^*$ character and are dominated by single excitations from the two highest occupied orbitals of the restricted Hartree–Fock (RHF) reference into the lowest-lying virtual orbital. We used these orbitals to generate a four-electron, three-orbital complete active space self-consistent field (CASSCF)¹³ wavefunction averaged¹⁴ over three states (SA3-CAS(4,3)). We used this to optimize S_0 and S_1 equilibrium geometries for all three forms, where we evaluated the S_0 , S_1 , and S_2 energies via multistate multireference Rayleigh–Schrödinger second-order perturbation theory (MS-MRPT2)^{15–17} with a Dunning double- ζ basis set with polarization functions on all atoms. At the S_0 configurations, these calculations predict S_0 – S_1 and S_0 – S_2 transitions at 4.04 and 4.91 eV (**CT-1**), 3.51 and 4.97 eV (**CT-2**), and 4.51 and 5.07 eV (**CA**). Corresponding excitations at the S_1 configurations were 3.99 and 4.90 eV (**CT-1**), 3.21 and 5.09 eV (**CT-2**), and 3.99 and 4.83 eV (**CA**). The S_0 energies for **CT-2** and **CA** were higher in energy than **CT-1** by 0.14 eV (3.2 kcal/mol) and 0.60 eV (13.8 kcal/mol), respectively, at the S_0 configurations. In the excited state, this situation is significantly altered, and the S_1 energy of **CT-2** is lower than that of both **CT-1** and **CA** by 0.54 eV (12.3 kcal/mol) and 1.46 eV

[†] Australian Institute for Bioengineering and Nanotechnology.

[‡] School of Physical Sciences.

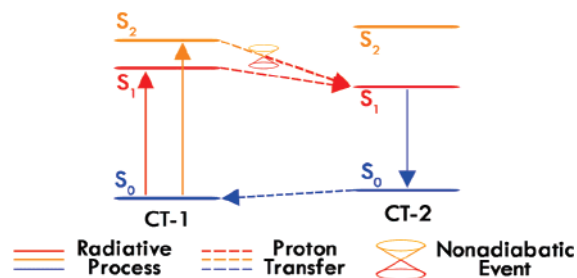


Figure 3. Dual ES IPT photocycle schematic. Energy levels are scaled to MS-MRPT energies. No barrier height information should be inferred.

(33.7 kcal/mol), respectively, at the S_1 geometries. The norm of the S_0 – S_1 difference dipole for **CT-2** is larger than that of **CT-1**, indicating a broadened transition within a simple Onsager model. RHF calculations in a conductor-like screening model (COSMO)¹⁸ of a dielectric environment indicated differential stabilization of **CA** relative to the catecholate forms that was of the same order as the MS-MRPT2 ground-state energy difference, consistent with coexistence of carboxylate and catecholate forms in solution.

These data led us to a photochemical reaction mechanism such as that in Figure 3. Within this mechanism, the dominant absorbing form is the catecholate anion **CT-1**. The dual absorption features can be attributed to the S_0 – S_1 and S_0 – S_2 transitions of **CT-1**. The resulting excited species react via adiabatic (S_1) or nonadiabatic (S_2) ES IPT to form the S_1 state of **CT-2**, which decays by photon emission. **CT-1** is regenerated on the ground state via the reverse reaction.

There may be significant population of the **CA** at pH 9.0. Our results suggest that the S_0 – S_1 transition of **CA** may contribute to the absorption at 4.2 eV, but that **CA** does not contribute to the emission. Photoexcited **CA** may form **CT-2** via multistep proton transfer with the solvent (in contrast to one-step internal transfer for **CT-1**). The close correspondence between the absorption and fluorescence excitation spectrum of DHICA at pH 9.0 suggests that the contribution of **CA** near 4.2 eV should be small (see Supporting Information). Accumulating populations of dianions may also contribute. The ratio of dianions to monoanions at pH 9.0 should be $10^{(pH-pK_a)} = 0.17$. DHICA may exist as three possible dianions. Exploratory MS-MRPT2 calculations suggest that similar ESPT processes exist within the dianionic population. The calculated oscillator strengths are generally lower than those for the monoanions.

We postulate the existence of a nonadiabatic pathway which forms the S_1 state of **CT-2** from the S_2 state of **CT-1**. We have verified this via the optimization of a minimal energy¹⁹ conical intersection characterized by intermediate O–H distances. Correlation of S_2 of **CT-1** and S_1 of **CT-2** is suggested by analysis of the orbital structure and the S_N – S_0 charge difference densities (see Supporting Information).

Reactions which transfer a light atom between two heavy atoms are known to be inherently multidimensional.²⁰ Barriers identified along one-dimensional reaction coordinates are of limited use in the analysis. Calculation of the full multidimensional reaction surface for proton transfer in DHICA will be the subject of future work.

Though we specifically address the photochemistry of DHICA, our results have profound implications within the broader context of melanin research. The broad absorbance of eumelanin is indicative of a dense manifold of states with varying degrees of localization.²¹ For eumelanin to fulfill its role as a photoprotectant, photoexcitations into many high-lying states must be funneled to fewer low-lying states in a manner that avoids chemical degradation of the pigment and/or surrounding tissue. The convergent ES IPT photocycles in DHICA fulfill this requirement, albeit on a much smaller scale. This raises the possibility that intramonomer ES IPT is a mechanism for energy dissipation from high-lying macromolecular states. To the best of our knowledge, this is a new suggestion within the melanin literature. We are pursuing further investigations.

Acknowledgment. We thank Dr. Jeff Reimers for very helpful discussions. Computations were performed at the APAC National Supercomputing Facility, Canberra. Time on the APAC machines was granted by Merit Allocation Scheme (MAS) and QCIF(QPSF) Partner-Share grants. Portions of this work were supported by a grant from the ARC/NHMRC Research Network “Fluorescence Applications in Biotechnology and the Life Sciences” (FABLS) and the by Australian Research Council (ARC). All quantum chemical calculations were performed with the MOLPRO²² software package.

Supporting Information Available: Complete citation for ref 22, sample preparation and characterization data, unscaled absorption and emission spectra, fluorescence excitation spectra, excitation dependence of the fluorescence, quantum yields, optimized Cartesian coordinates in angstroms, absolute energies, dipole moments, and state-averaged active orbitals and occupation numbers. This material is available free of charge via the Internet at <http://pubs.acs.org>.

References

- (1) Klessinger, M.; Michl, J. *Excited States and Photochemistry of Organic Molecules*; VCH: New York, 1995.
- (2) Prota, G. *Melanins and Melanogenesis*; Academic Press: New York, 1992.
- (3) Meredith, P.; Sarna, T. *Pigment Cell Res.* **2006**, *19* (6), 572–594.
- (4) Nofsinger, J. B.; Ye, T.; Simon, J. D. *J. Phys. Chem. B* **2001**, *105* (14), 2864–2866.
- (5) Meredith, P.; Riesz, J. *Photochem. Photobiol.* **2004**, *79* (2), 211–216.
- (6) Nofsinger, J. B.; Weinert, E. E.; Simon, J. D. *Biopolymers* **2002**, *67* (4–5), 302–305.
- (7) Meredith, P.; Powell, B. J.; Riesz, J.; Nighswander-Rempel, S. P.; Pederson, M. R.; Moore, E. G. *Soft Matter* **2006**, *2* (1), 37–44.
- (8) Charkoudian, L. K.; Franz, K. J. *Inorg. Chem.* **2006**, *45* (9), 3657–3664.
- (9) Onufriev, A.; Case, D. A.; Ullman, G. M. *Biochemistry* **2001**, *40* (12), 3414–3419.
- (10) Stanton, J. F.; Bartlett, R. J. *J. Chem. Phys.* **1993**, *98* (9), 7029–7039.
- (11) Dunning, T. H.; Hay, P. J. In *Methods of Electronic Structure Theory*; Schaefer, H. F., Ed.; Plenum Press: New York, 1977; Vol. 2.
- (12) Dunning, T. H. *J. Chem. Phys.* **1970**, *53*, 2823.
- (13) Roos, B. O.; Taylor, P. R.; Siegbahn, P. E. M. *Chem. Phys.* **1980**, *48* (2), 157–173.
- (14) Docken, K. K.; Hinze, J. J. *J. Chem. Phys.* **1972**, *57* (11), 4928–4936.
- (15) Werner, H.-J. *Mol. Phys.* **1996**, *89* (2), 645–661.
- (16) Finley, J.; Malmqvist, P.-A.; Roos, B. O.; Serrano-Andres, L. *Chem. Phys. Lett.* **1998**, *288* (2–4), 299–306.
- (17) Celani, P.; Werner, H.-J. *J. Chem. Phys.* **2000**, *112* (13), 5546–5557.
- (18) Klamt, A.; Schüürmann, G. *J. Chem. Soc., Perkin Trans. 2* **1993**, 799–803.
- (19) Bearpark, M. J.; Robb, M. A.; Bernhard Schlegel, H. *Chem. Phys. Lett.* **1994**, *223* (3), 269–274.
- (20) Carrington, T. J.; Miller, W. H. *J. Chem. Phys.* **1986**, *84* (8), 4364–4370.
- (21) Tran, M. L.; Powell, B. J.; Meredith, P. *Biophys. J.* **2006**, *90* (3), 743–752.
- (22) Werner, H. J.; et al. *MOLPRO* 2006.1, 2006.

JA069280U